

# Theory and Implementation of 2.5D WFS of moving sources with arbitrary trajectory

Gergely Firtha, Péter Fiala

<sup>1</sup> *Budapest University of Technologies and Economics, 1117 Budapest, Hungary, Email: firtha,fiala@hit.bme.hu*

## Introduction

Wave Field Synthesis (WFS) aims at the reconstruction of the physical properties of a target sound field over an extended listening area using a densely spaced loudspeaker ensemble, termed the secondary source distribution (SSD). The loudspeakers are driven with driving signals, ensuring that the resultant field of the SSD coincides with the target sound field. Traditionally the driving signals are extracted from an appropriate boundary integral representation of the target field [1]. As an alternative approach, the same driving functions are obtained by applying a high-frequency approximation to the explicit solution of the corresponding inverse integral problem [2].

In the aspect of reproducing dynamic sound scenes the synthesis of the field generated by a moving point source is of particular interest and is well studied in the related literature [3, 4]. Recently a WFS approach was presented by the present authors for the synthesis of a moving source with an arbitrary shaped SSD, ensuring optimal synthesis over a prescribed *reference curve* [5].

The practical implementation of this solution, however, raises a number of questions: several variables present in the driving functions—e.g. the source trajectory and position at the emission time along with the referencing distance—are assumed to be known a-priori, while the actual evaluation of these quantities leads to numerical problems.

Furthermore, the presented driving functions assume a continuous SSD, while practical implementations apply a finite number of closely spaced loudspeakers, leading to *spatial aliasing artifacts*. These clearly audible artifacts are more enhanced in the present dynamic scenario than in case of the synthesis of a static virtual field [3, 6].

The present contribution investigates the practical implementation of the 2.5D WFS driving functions applying a life-like, discrete loudspeaker array.

## Theoretical basics

Assume a virtual point source moving along an arbitrary trajectory, with the time-dependent source position described by  $\mathbf{x}_s(t) = [x_t(t), y_s(t), 0]^T$ ! The source is radiating with the excitation time history  $s(t)$ . The trajectory is restricted to the horizontal plane  $z = 0$  in order to ensure that an SSD located in the same plane may achieve a phase correct synthesis in the listening area. The arbitrary shaped, smooth, convex and theoretically continuous distribution of secondary point sources are located at  $\mathbf{x}_0 = [x_0, y_0, 0]^T$ .

The time domain driving function for the synthesis of the moving point source with a wideband excitation signal

reads as [5]

$$d(\mathbf{x}_0, t) = w(\mathbf{x}_0, t) \sqrt{d_{\text{ref}}(\mathbf{x}_0, t)} \sqrt{\frac{1}{2\pi c}} \cdot \langle \mathbf{x}_0 - \mathbf{x}_s(t - \tau(\mathbf{x}_0, t)) \cdot \mathbf{n}_{\text{in}}(\mathbf{x}_0) \rangle \frac{s'_t(t - \tau(\mathbf{x}_0, t))}{\Delta(\mathbf{x}_0, t - \tau(\mathbf{x}_0, t))^{\frac{3}{2}}}, \quad (1)$$

where the prefiltered input signal is given by  $s'_t(t) = h(t) * s(t)$ , with the pre-equalization filter's impulse response given by  $h(t) = \mathcal{F}_t^{-1} \{ \sqrt{j\omega} \}$ .

In the driving function  $\tau(\mathbf{x}_0, t)$  describes the propagation time delay, satisfying the quadratic equation

$$\tau(\mathbf{x}_0, t) = \frac{|\mathbf{x}_0 - \mathbf{x}_s(t - \tau(\mathbf{x}_0, t))|}{c}, \quad (2)$$

describing the time which the wavefronts of the virtual source requires to reach the actual SSD elements, while

$$\Delta(\mathbf{x}_0, t) = |\mathbf{x}_0 - \mathbf{x}_s(\mathbf{x}_0, t)| - \left\langle \frac{\mathbf{v}_s(\mathbf{x}_0, t)}{c} \cdot (\mathbf{x}_0 - \mathbf{x}_s(\mathbf{x}_0, t)) \right\rangle \quad (3)$$

describes the spatial amplitude distribution, generated by a moving source, with  $\mathbf{v}_s(\mathbf{x}_0, t) = \frac{d}{dt} \mathbf{x}_s(\mathbf{x}_0, t)$  being the source velocity.

The time-domain referencing function, allowing the optimization of synthesis on a prescribed reference curve  $C_{\text{ref}}$  reads as

$$d_{\text{ref}}(\mathbf{x}_0, t) = \frac{|\mathbf{x}_{\text{ref}}(\mathbf{x}_0, t) - \mathbf{x}_0|}{|\mathbf{x}_{\text{ref}}(\mathbf{x}_0, t) - \mathbf{x}_0| + |\mathbf{x}_0 - \mathbf{x}_s(t - \tau(\mathbf{x}_0, t))|} \quad (4)$$

with  $\mathbf{x}_{\text{ref}}(\mathbf{x}_0, t) \in C_{\text{ref}}$  being the reference position for a given SSD element. Finally one may introduce the local wavenumber vector, defined for a harmonic source excitation at  $\omega_0$  reading

$$\mathbf{k}^P(\mathbf{x}_0, t) = \frac{\omega(\mathbf{x}_0, t)}{c} \frac{\mathbf{x}_0 - \mathbf{x}_s(t - \tau(\mathbf{x}_0, t))}{|\mathbf{x}_0 - \mathbf{x}_s(t - \tau(\mathbf{x}_0, t))|}, \quad (5)$$

where  $\omega(t)$  is the perceived, measured angular frequency, altered by the Doppler effect.

## Implementation of WFS driving functions

The above WFS driving functions theoretically ensure the perfect reproduction of the field of a moving source over the reference curve, and phase correct synthesis inside the listening area. However their implementation is not straightforward, both the definition of the source trajectory, the definition of the corresponding propagation time delays and the calculation of the referencing functions are computationally expensive. Furthermore, practical WFS

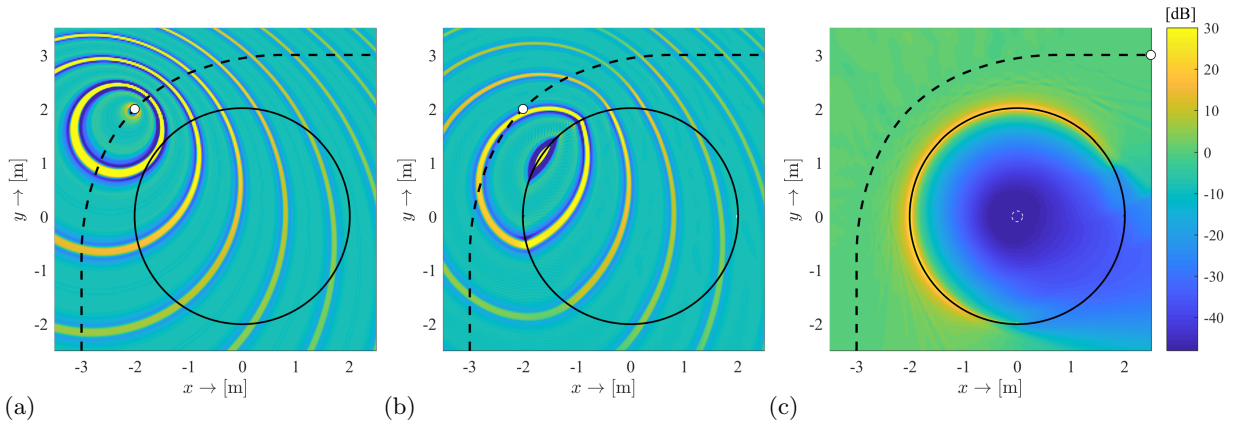


**Figure 1:** Reproduction of a moving source along an arbitrary path, defined as a smoothed polyline with user-defined anchor points. The source travels along the path with a constant velocity  $v = 200$  m/s, with both the source trajectory and the propagation time delays evaluated numerically for each field point and SSD element by using the presented approaches. The source emits a series of temporally bandlimited impulses and the synthesis is referenced to the center of the circular SSD with  $R_{\text{SSD}} = 2$  m. Figure (a) shows the target sound field, figure (b) shows the synthesized field at  $t \approx 25$  ms. Figure (c) shows the cumulated relative error in a logarithmic scale, calculated as  $\int_0^T (P(\mathbf{x}, t) - P_{\text{synth}}(\mathbf{x}, t))^2 dt / \int_0^T P(\mathbf{x}, t)^2 dt$ .

setups employ a finite number of extended loudspeakers opposed to the theoretical continuous SSD, resulting in spatial aliasing artifacts, which have to be taken into consideration. In the followings efficient computation schemes and the possibilities for optimal antialiasing filtering are discussed.

**Calculation of the the source trajectory:** Direct implementation of the moving source driving function (1) assumes that the time dependence of the source position  $\mathbf{x}_s(t)$  is known a-priori, which is an optimistic assumption in the aspect of practical applicability. Instead, more often a parametric curve  $\mathbf{y}(p)$  is given, which the virtual source follows with a pre-defined velocity profile. This requirement can be formulated as finding a reparameterization, so that

$$\mathbf{y}(p(t)) = \mathbf{x}_s(t), \quad \left| \frac{d\mathbf{x}_s(t)}{dt} \right| = |\mathbf{v}_s(t)| \quad (6)$$

holds. The goal is to find the explicit parametrization  $p(t)$  so that substitution into (6) yields the desired source position vector.

Differentiation of (6) with respect to time and application of the chain rule results in the following expression of  $dp/dt$ :

$$\frac{dp(t)}{dt} = \frac{|\mathbf{v}_s(t)|}{|d\mathbf{y}(p(t))/dp|}. \quad (7)$$

The parametrization  $p(t)$  is then obtained by integration:

$$p(t) = \int_{t_0}^t \frac{|\mathbf{v}_s(s)|}{|d\mathbf{y}(p(s))/dp|} ds \quad (8)$$

with  $t_0$  being a user-defined initial time. Note that for sources moving with constant velocity ( $|\mathbf{v}_s(s)| = v$ ) the parametrization is referred to as reparameterization to arc-length.

For an arbitrary trajectory and velocity profile the parametrization (8) can only be evaluated numerically. A detailed discussion on the frequently used numerical methods can be found in [7]. As a simplest approach,

the integral may be approximated numerically with the forward-Euler method, approximating the integral with the iteration scheme

$$p_{i+1} = p_i + dt \frac{|\mathbf{v}_s(p_i)|}{|d\mathbf{y}(p_i)/dp|}, \quad i \geq 0, \quad (9)$$

where  $dt = \frac{1}{f_s}$  is the sampling period of the source trajectory. Once the parametrization  $p_i$  is found, the required source trajectory vector at the time instant  $t_i$  can be obtained from  $\mathbf{x}_s(t_i) = \mathbf{y}(p_i)$ .

**Calculation of the retarded time and source position:** Having found the source trajectory the implementation of the driving functions would still require the solution of the quadratic equation (2) for each SSD element at each time instant, in order to find the propagation time delay between the moving source at the emission time  $t - \tau$  and the SSD elements at the receiving time, which makes real-time implementation infeasible.

The computational complexity may be considerably decreased by implementing a further Euler iteration scheme, i.e. by approximating  $\tau(\mathbf{x}, t)$  by its first order Taylor series

$$\tau(\mathbf{x}, t + dt) \approx \tau(\mathbf{x}, t) + dt \frac{d\tau(\mathbf{x}, t)}{dt}, \quad (10)$$

with the temporal derivative of  $\tau$  obtained from the implicit derivation of its definition (2), reading as

$$\frac{d\tau(\mathbf{x}, t)}{dt} = \tau'(\mathbf{x}, t) = \frac{-\frac{1}{c} \langle \mathbf{v}_s(t - \tau) \cdot (\mathbf{x} - \mathbf{x}_s(t - \tau)) \rangle}{|\mathbf{x} - \mathbf{x}_s(t)|}. \quad (11)$$

Hence the iteration scheme at the time instant  $t_i$  reads as

$$\tau(\mathbf{x}, t_i) = \tau(\mathbf{x}, t_{i-1}) + dt \cdot \tau'(\mathbf{x}, t_{i-1}), \quad (12)$$

with  $dt = \frac{1}{f_s}$  being the sampling period of the driving function [5]. Obviously, when only numerically available,  $\mathbf{x}_s(t - \tau)$  may be interpolated from the trajectory vector, from which the source velocity  $\mathbf{v}_s(t - \tau)$  may be calculated by differentiating it numerically with respect to time.

It is important to note that the sampling frequency

for the calculation of the source trajectory and propagation time delay may be chosen significantly lower than the actual source driving signal's sampling frequency. As a result computational cost can be decreased, besides still ensuring numerical stability.

**Choosing the referencing scheme:** Evaluation of the driving functions (1) require the definition of a desired referencing scheme as it is discussed in details in [8]: a reference curve  $C_{\text{ref}}$  has to be prescribed inside the listening area, at which the driving functions ensure amplitude correct synthesis. Calculating the driving functions then requires the definition of the reference position  $\mathbf{x}_{\text{ref}}(\mathbf{x}_0, t)$  for each SSD element at each time instant as the point, satisfying  $\hat{\mathbf{k}}^P(\mathbf{x}_0, t) = \hat{\mathbf{k}}^G(\mathbf{x}_{\text{ref}}(\mathbf{x}_0, t) - \mathbf{x}_0)$ , with  $\mathbf{x}_{\text{ref}}(\mathbf{x}_0, t) \in C_{\text{ref}}$  and  $\hat{\mathbf{k}}$  being the frequency-dependent normalized wavenumber vector, pointing into the local propagation direction of a sound field. In practice this point is found at the intersection of a straight line—connecting the actual SSD element  $\mathbf{x}_0$  with the corresponding source position at the emission time  $\mathbf{x}_s(t - \tau(\mathbf{x}_0, t))$ —and a polyline, defining reference curve.

Obviously, the direct solution for the reference position is of great computational cost, making real-time applications infeasible. As a possible solution specific reference curve shapes may be used for which the analytical solution for the reference position is available. As an example, in case of circular SSDs the choice of a concentric circle for the reference curve may be feasible, for which geometry the intersection of a parametric line and a circle is well-known [9, Ch.7.3.2]. However, as a result amplitude correct synthesis at a given time instant is ensured only over an arc, for which part of the reference curve a stationary SSD element exist.

Alternatively, as the most simple solution, synthesis may be optimized to a given reference point  $\mathbf{x}_{\text{ref}}$  independently from the actual SSD position, e.g. to the center of the SSD in case of a circular secondary ensemble. Since ideal antialiasing can be also achieved only at a given listening position, this simple choice may be feasible in the aspect of practical implementation.

An implementation of the presented numerical and referencing solutions for the synthesis of a moving point source is presented in Figure 1, verifying that referencing the synthesis to the center of a circular secondary array ensures an amplitude correct synthesis over the entire virtual source pass-by in that position.

**Avoiding spatial aliasing:** So far the implementation of WFS driving functions applying a continuous SSD was investigated. In practice sound field synthesis is performed by applying a set of loudspeakers at discrete positions, leading to clearly audible *spatial aliasing artifacts*. These artifacts manifest in a series of echoes behind the primary/virtual wave front in the synthesized field: these secondary wavefronts—the spherical wavefronts of the individual SSD elements—can not be canceled above a given angular frequency due to the finite loudspeaker spacing, which cancellation would be ensured by the half-differentiator characteristics of the driving function in the theoretical continuous case. The spatial aliasing artifacts

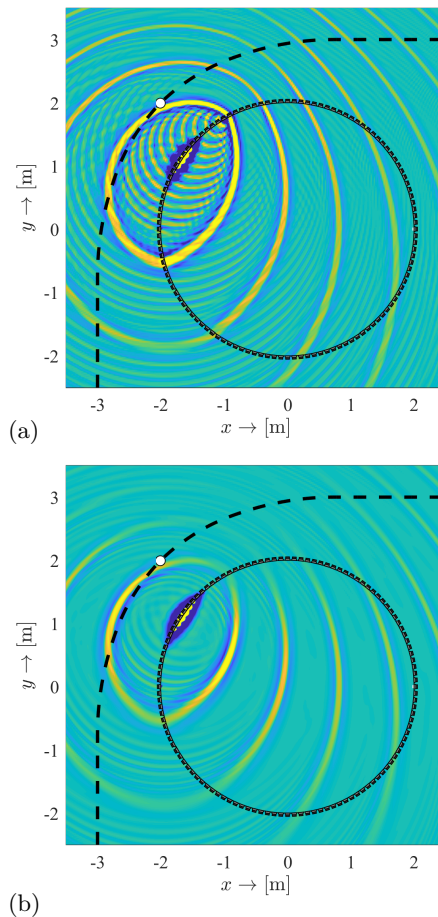


**Figure 2:** Synthesis of the moving source with the same simulation setup as used in Figure 1, by using a discrete set of 120 loudspeakers. Figure (a) shows the effects of source discretization with clearly visible aliasing echoes in front of the virtual source, where the local perceived frequency is increased by the Doppler effect. Figure (b) shows the effect of ideal antialiasing filtering the driving functions by temporal lowpass filtering under the time-variant cut-off frequency (16) in the Short-time Fourier Transform domain with properly chosen window and hop sizes.

are even more emphasized in case of the synthesis of a moving virtual point source, since the aliasing echo components suffer a different Doppler shift than the primary wavefront, resulting in strong spectral coloration [6]

The effects of the SSD discretization can be investigated analytically in the wavenumber domain for the special case of an infinite linear SSD [1]. In this case the spectral representation of an arbitrary synthesized field is yielded as the product of the spectrum of the discrete driving function sampled at the actual loudspeaker positions and the Green's function, representing the field of the individual loudspeakers

$$\tilde{P}(k_x, y, \omega) = \tilde{G}(k_x, y, \omega) \sum_{n=-\infty}^{\infty} \tilde{D}(k_x - n \frac{2\pi}{\Delta x}, \omega), \quad (13)$$

where  $\Delta x$  is the loudspeaker spacing.

In the synthesized field spatial-aliasing components are present due to the overlapping in the repetitive driving function spectrum. Hence, for a linear SSD aliasing (spectral overlapping) is avoided by bandlimiting the driving

function to the Nyquist wavenumber, i.e. by ensuring that

$$\tilde{D}(k_x, \omega) = 0, \quad \text{for } k_x > \frac{\pi}{\Delta x} \quad (14)$$

holds.

In a recent paper by the present authors it was proven that a given wavenumber component  $k_x$  in the spectrum of the driving function is dominated by those locations  $\mathbf{x}_0$ , where the local wavenumber vector of the virtual field coincides with the that of the spectral plane wave described by  $k_x$ , i.e. where  $k_x^P(\mathbf{x}_0) = k_x$  holds [2].

This important statement allows one to introduce an antialiasing condition in the spatial domain.

$$D(\mathbf{x}_0, \omega) = 0, \quad \text{for } k_t^P(\mathbf{x}_0) > \frac{\pi}{\Delta x}. \quad (15)$$

Here  $k_t$  denotes the tangential component of the local wavenumber vector: within the validity of the Kirchhoff approximation a smooth SSD curve may be considered locally linear, and the linear driving functions may be applied locally. In this general case the  $k_x$  component is changed to the tangential component of the local wavenumber vector.

For the case of a moving point source the local wavenumber vector is given by (5) as the function of the perceived angular frequency. Hence the antialiasing condition can be formulated as band-limiting the driving functions to the angular frequency

$$\omega_c(\mathbf{x}_0, t) > \frac{\pi c}{\Delta x} \frac{|\mathbf{x}_0 - \mathbf{x}_s(t - \tau(\mathbf{x}_0, t))|}{\langle \mathbf{x}_0 - \mathbf{x}_s(t - \tau(\mathbf{x}_0, t)) \cdot \mathbf{t}(\mathbf{x}_0) \rangle}. \quad (16)$$

This means that antialiasing requires the implementation of a time varying low pass filter with the cut-off frequency given above.

Practically as a result full-band synthesis is achieved only on those parts of the synthesized field, for which the stationary SSD element's normal vector coincides with the local propagation direction of the virtual field. For the special case of a circular SSD due to the geometry at the center of the SSD the existence of a nearly full-band stationary SSD element is inherently ensured, hence in the center position nearly full-band antialiased synthesis may be achieved. Terminology nearly full-band synthesis refers to that since due to discretization of the SSD full-band synthesis is only possible when at the stationary SSD position an actual SSD element is located. Hence in practice when the moving source is located between two SSD elements even at the center of the array the synthesized field is bandlimited which may cause audible effects if the source is close to the SSD.

The result of the proposed antialiasing approach is illustrated in Figure 2 in case of a circular SSD. The simulation results verify the nearly full-band synthesis in the center of the secondary array.

## Conclusion

The present contribution dealt with the questions arising at the practical implementation of the Wave Field Synthesis of moving point sources. Numerical schemes were proposed, allowing the real-time evaluation of the required WFS driving function. Furthermore a simple and efficient

anti-aliasing strategy was presented, realizing local Wave Field Synthesis by optimizing the anti-aliased synthesis to a particular area in the listening space. This latter solution involves the application of non-stationary filtering requiring space-dependent low-pass filtering of the driving functions with an analytically given cut-off frequency.

Obviously, truly real-time/online application of the approach requires the implementation of non-stationary convolution for both the non-stationary retardation of the excitation signal present in the driving function (1) and proper anti-aliasing filtering. This aspect is however out of the scope of the present treatise.

The presented solutions are implemented in MATLAB environment generating loudspeaker driving functions for a circular SSD along with configuration files for the SOUNDSCAPE RENDERER [10] and is freely available for download at [https://github.com/gfirtha/DAGA2018\\_moving\\_sources](https://github.com/gfirtha/DAGA2018_moving_sources).

## Acknowledgement



Supported by the ÚNKP-17-3-IV New National Excellence Program of the Ministry of Human Capacities

## References

- [1] J. Ahrens. *Analytic Methods of Sound Field Synthesis*. Springer, Berlin, 1st edition, 2012.
- [2] G. Firtha and P. Fiala. The general relation of wave field synthesis and the spectral division method. *IEEE Trans. Audio, Speech, Lang. Process.*, 2018. Submitted for peer-review.
- [3] A. Franck, A. Graefe, K. Thomas, and M. Strauss. Reproduction of Moving Sound Sources by Wave Field Synthesis: An Analysis of Artifacts. In *Proc. of the 32nd Intl. Conf. Audio Eng. Soc.: DSP For Loudspeakers*, Hillerod, Sept. 2007.
- [4] J. Ahrens and S. Spors. Reproduction of Moving Virtual Sound Sources with Special Attention to the Doppler Effect. In *Proc. of the 124th Audio Eng. Soc. Convention*, Amsterdam, May 2008.
- [5] G. Firtha and P. Fiala. Wave field synthesis of moving sources with arbitrary trajectory and velocity profile. *The Journal of the Acoustical Society of America*, 142(2):551–560, 2017.
- [6] G. Firtha and P. Fiala. Investigation of spatial aliasing artifacts of wave field synthesis for the reproduction of moving virtual point sources. In *in 42nd German Annual Conference on Acoustics (DAGA)*, pages 1008–1011, Aachen, Germany, Mar. 2016.
- [7] R. Parent. *Computer Animation*. Morgan Kaufmann, 3rd edition, 2012.
- [8] G. Firtha, P. Fiala, F. Schultz, and S. Spors. Improved referencing schemes for 2.5d wave field synthesis driving functions. *IEEE/ACM Trans. Audio, Speech, Lang. Process.*, 25(5):1117–1127, May 2017.
- [9] P.J. Schneider D. H. Eberly. *Geometric Tools for Computer Graphics*. Elsevier, 2003.
- [10] J. Ahrens, M. Geier, and S. Spors. The soundscape renderer: A unified spatial audio reproduction framework for arbitrary rendering methods. In *Audio Engineering Society Convention 124*, May 2008.